32. Ab BK, Kiessling R, Van Embden JD, Thole JE, Kumararatne DS, Pisa P, Wondimu A, Ottenhoff TH (1990) Induction of antigen-specific CD4+ HLA-DR-restricted cytotoxic T lymphocytes as well as nonspecific nonrestricted killer cells by the recombinant mycobacterial 65-kDa heat-shock protein. Eur J Immunol 20(2):369–377. doi:10.1002/eji.1830200221

33. Bourgault I, Gomez A, Gomard E, Picard F, Levy JP (1989) A virus-specific CD4+ cell-mediated cytolytic activity revealed by CD8+ cell elimination regularly develops in uncloned human antiviral cell lines. J Immunol 142(1):252–256

PLOS ONE

Ectopic Fat Accumulation and Distant Organ-Specific Insulin Resistance in Japanese People with Nonalcoholic Fatty Liver Disease

Ken-ichiro Kato[1☯], Toshinari Takamura[1*☯], Yumie Takeshita[1], Yasuji Ryu[2], Hirofumi Misu[1], Tsuguhito Ota[1], Kumpei Tokuyama[3], Shoichiro Nagasaka[4], Munehide Matsuhisa[5], Osamu Matsui[2], Shuichi Kaneko[1]

1 Department of Disease Control and Homeostasis, Kanazawa University Graduate School of Medical Sciences, Kanazawa, Ishikawa, Japan, **2** Department of Radiology, Kanazawa University Graduate School of Medical Sciences, Kanazawa, Ishikawa, Japan, **3** Graduate School of Comprehensive Human Science, University of Tsukuba, Tsukuba, Ibaraki, Japan, **4** Department of Medicine, Division of Endocrinology and Metabolism, Jichi Medical University, Shimono, Tochigi, Japan, **5** Clinical Research Center for Diabetes, Tokushima University, Tokushima, Tokushima, Japan

Abstract

Objective: The aim of this study was to examine the association between ectopic fat and organ-specific insulin resistance (IR) in insulin-target organs in patients with nonalcoholic fatty liver disease (NAFLD).

Methods: Organ-specific IR in the liver (hepatic glucose production (HGP)×fasting plasma insulin (FPI) and suppression of HGP by insulin [%HGP]), skeletal muscle (insulin-stimulated glucose disposal [Rd]), and adipose tissue (suppression of FFA by insulin [%FFA]) was measured in 69 patients with NAFLD using a euglycemic hyperinsulinemic clamp with tracer infusion ([6,6-$^2H_2$]glucose). Liver fat, intramyocellular lipid (IMCL), and body composition were measured by liver biopsy, proton magnetic resonance spectroscopy, and bioelectrical impedance analysis, respectively.

Results: HGP×FPI was significantly correlated with Rd ($r=-0.57$, $P<0.001$), %HGP with %FFA ($r=0.38$, $P<0.01$), and Rd with %FFA ($r=0.27$, $P<0.05$). Liver steatosis score was negatively associated with Rd ($r=-0.47$, $P<0.001$) as well as with HGP×FPI ($r=0.43$, $P<0.001$). Similarly, intrahepatic lipid was negatively associated with Rd ($r=-0.32$, $P<0.05$). IMCL was not associated with Rd ($r=-0.16$, $P=0.26$). Fat mass and its percentage were associated with HGP×FPI ($r=0.50$, $P<0.001$; $r=0.48$, $P<0.001$, respectively) and Rd ($r=-0.59$, $P<0.001$; $r=-0.52$, $P<0.001$, respectively), but not with %FFA ($r=-0.21$, $P=0.10$; $r=-0.001$, $P=0.99$, respectively).

Conclusion: Unexpectedly, fat accumulation in the skeletal muscle and adipose tissue was not associated with organ-specific IR. Instead, liver fat was associated not only with hepatic IR but also with skeletal muscle IR, suggesting a central role of fatty liver in systemic IR and that a network exists between liver and skeletal muscle.

Citation: Kato K-i, Takamura T, Takeshita Y, Ryu Y, Misu H, et al. (2014) Ectopic Fat Accumulation and Distant Organ-Specific Insulin Resistance in Japanese People with Nonalcoholic Fatty Liver Disease. PLoS ONE 9(3): e92170. doi:10.1371/journal.pone.0092170

Editor: Yanqiao Zhang, Northeast Ohio Medical University, United States of America

Received December 29, 2013; **Accepted** February 18, 2014; **Published** March 20, 2014

Funding: This work was supported in part by a grant-in-aid for Scientific Research (C-20591054 to TT) from the Ministry of Education, Culture, Sports, Science, and Technology, Japan. The funders had no role in study design, data collection and analysis, decision to publish, or preparation of the manuscript. No additional external funding received for this study.

Competing Interests: The authors have declared that no competing interests exist.

* E-mail: ttakamura@m-kanazawa.jp

☯ These authors contributed equally to this work.

Introduction

Insulin resistance (IR) is a core pathology of type 2 diabetes mellitus (T2DM), nonalcoholic fatty liver disease (NAFLD), and cardiovascular diseases [1–3]. The severity of IR may differ among the major insulin-target organs, the liver, skeletal muscle, and adipose tissue [4]. Accumulating evidence suggests that ectopic fat accumulation in insulin-target organs leads to development of IR in each organ by altering oxidative stress [5–7] and gene expression profiles [8,9]. Indeed, liver steatosis is associated with whole-body IR, independently of body mass index (BMI) [10].

Conversely, inter-organ network and organ-derived bioactive hormones such as adiponectin and selenoprotein P may play a role in the development of distant organ IR [11–13]. Therefore, to understand organ networks that sense excess energy and regulate insulin action, elucidating the association between fat accumulation and organ-specific IR among the liver, skeletal muscle, and adipose tissue is important, especially in humans. However, no previous studies have demonstrated the association among these organs comprehensively and simultaneously [14,15]. In addition, liver biopsy remains gold standard for diagnosis of NAFLD because it more accurately measures liver fat than proton

magnetic resonance spectroscopy (^{1}H-MRS) under some conditions [16].

The present study try to address the association of organ-specific IR with ectopic fat among the liver, skeletal muscle, and adipose tissue in Japanese patients with NAFLD, systematically using reliable methods including liver biopsy, assessment of glucose metabolism measured by a euglycemic hyperinsulinemic clamp study with stable-isotope, and ^{1}H-MRS.

Materials and Methods

Ethics Statement

The study was approved by the Medical Ethics Committee of Kanazawa University (Approval No. 845), and written informed consent was obtained from each patient prior to participation. The study was conducted in accordance with the Declaration of Helsinki.

Participants and Study Design

We studied 69 patients clinically diagnosed with NAFLD, recruited consecutively between 2010 and 2012 from Kanazawa University Hospital, Japan. The patients were in good general health without evidence of any acute or chronic diseases (other than NAFLD, T2DM, hypertension, or dyslipidemia) as determined by history, physical examination, routine blood chemistries, urinalysis, and electrocardiography. Out of the 69 patients, 37 (54%) had T2DM according to the American Diabetes Association criteria. Of the 37 T2DM patients, antidiabetic agents were administered to 18 patients in monotherapy and 7 patients in combination therapy (metformin, n = 15; dipeptidyl peptidase-4 inhibitors, n = 9; glucagon-like peptide-1 agonists, n = 7; mealtime dosing of a rapid-acting insulin analog, n = 5, respectively). None of the patients were taking α-glucosidase inhibitors, rapid-acting insulin secretion agents, sulfonylurea, thiazolidinediones, or long-acting insulin. Participants were excluded if they had a history of alcohol abuse (more than 20 g/day), liver diseases other than NAFLD (hepatitis B or C, autoimmune hepatitis, hemochromatosis, Wilson disease, drug-induced disease, or other), type 1 diabetes, or a history of clinically significant renal, pulmonary, or heart diseases.

The participants were studied on four separate occasions. Generally, all measurements were performed within 1 month and included: 1) organ-specific IR in the liver, skeletal muscle, and adipose tissue by a euglycemic hyperinsulinemic clamp study with tracer ([6,6-$^2H_2$]glucose) infusion; 2) liver biopsy for histology to confirm the diagnosis of NAFLD and score the degree of steatosis, grade, and stage; 3) intrahepatic lipid (IHL) and intramyocellular lipid (IMCL) measured by ^{1}H-MRS, and body composition by a bioelectrical impedance analysis; and 4) 75-g oral glucose tolerance test (OGTT) to evaluate the glucose tolerance according to American Diabetes Association criteria [17].

Euglycemic Hyperinsulinemic Clamp

After an overnight fast, two intravenous catheters, one for blood sampling and one for infusion of glucose, insulin, and tracers, were inserted in the antecubital vein of each arm. At 0700 h, after obtaining a blood sample for background enrichment of plasma glucose, a continuous infusion of [6,6-$^2H_2$]glucose (>99% enriched; Cambridge Isotope, Andover, MA, USA) was started at a rate of 0.05 mg·kg^{-1}·min^{-1} after a priming dose equivalent. After 100, 110, and 120 min, blood samples were obtained for determination of tracer enrichments. Subsequently, at 0900 h, the euglycemic hyperinsulinemic clamp study was started using an artificial pancreas (model STG-55; Nikkiso, Tokyo, Japan), as described previously [18,19]. A primed continuous infusion of insulin (Humulin R; Eli Lilly, Indianapolis, IN, USA) was started for 2.0 h at a rate of 1.25 mU·kg^{-1}·min^{-1} to attain a plasma insulin concentration of approximately 100 μU/mL. Glucose was infused to maintain a plasma glucose concentration of 100 mg/dL (or 90 mg/dL for baseline values under 90 mg/dL). Simultaneously, [6,6-$^2H_2$]glucose infusion was continued at a rate of 0.15 mg·kg^{-1}·min^{-1}. During the last 20 min of the clamp study, blood samples were obtained in 10-min intervals to determine tracer enrichments.

Liver Biopsy/Pathology

Ultrasound-guided liver biopsy specimens were obtained from all 69 patients. Each specimen was stained with hematoxylin-eosin and silver reticulin stains and histologically examined by one experienced pathologist who was blinded to the patient's clinical condition and biochemical data. The biopsied tissues were scored for steatosis (0, none; 1, <33%; 2, 33–66%; 3, >66%), stage, and grade as described previously (10), according to the standard criteria for grading and staging of nonalcoholic steatohepatitis proposed by Brunt et al. [20,21].

Liver Fat Content and IMCL (Proton Magnetic Resonance Spectroscopy)

IHL and IMCL were measured as reported previously [22,23]. Briefly, IHL of the liver's right lobe and IMCL of the soleus muscle were measured by ^{1}H-MRS using a whole-body 3.0 T MR System (Signa HDxt 3.0 T, General Electric Healthcare, Milwaukee, WI, USA). Voxels (3.0×3.0×3.0 cm^3 for liver and 2.0×2.0×2.0 cm^3 for soleus muscle) were positioned in the liver or soleus muscle to avoid blood vessels and visible interfacial fat, and the voxel sites were carefully matched at each examination. Imaging parameters were set to repetition time of 1500 ms and echo time of 27 ms. To quantify IHL and IMCL, the MR spectral raw data were processed by using the LCModel software (Version 6.3-0C, Stephen Provencher, Oakville, Ontario, Canada).

Body Composition

Body composition, such as fat mass and fat-free mass, was determined by a bioelectrical impedance analysis (Tanita BC-118D, Tanita, Tokyo, Japan).

Oxygen Consumption

Oxygen consumption was measured using indirect calorimetry (Aeromonitor AE310S, Minato, Osaka, Japan).

75-g OGTT

After an overnight fast, a 75-g OGTT was performed at 0800 h. Blood samples were collected at 0, 30, 60, 90, 120, and 180 min to measure plasma glucose insulin and C-peptide concentrations.

Analytical Methods

Plasma glucose was measured by the glucose oxidase method (Glucose Analyzer GA09; A&T, Kanagawa, Japan), and plasma insulin and C-peptide were measured using a sandwich enzyme immunoassay system with E-test Tosoh II (IRI) and E-test Tosoh II (C-peptide) (Tosoh, Tokyo, Japan). Plasma FFA was measured by a standard colorimetric method using NEFA-SS (Eiken, Tokyo, Japan). Hemoglobin A1c level was measured using high-performance liquid chromatography (TOSOH HLC-723G8; Tosoh, Tokyo, Japan).

Deuterated glucose was analyzed as a penta-acetate derivative using the method by Wolfe [24]. Samples were analyzed on a

quadrupole gas chromatography mass spectrometry instrument (GCMS-QP1100EX, Shimadzu, Kyoto, Japan) operated in the electron impact mode by selective-ion monitoring of m/z 200, 201, and 202. Oven temperature was 180°C with a 10°C/min rate of temperature rise until 250°C with a 25 m HR-1 capillary column (Shinwa Chemical Industries, Kyoto, Japan). Tracer concentrations were calculated based on the sample's tracer-to-tracee mass ratio [25].

Calculations

In the basal state, hepatic glucose production (HGP) was calculated as the rate of appearance (Ra) of glucose according to the Steele's equation as previously described [19,26]. During the clamp study, glucose Ra was calculated using Steele's equation from tracer data [26]. HGP during the clamp study was calculated as the difference between glucose Ra and the infusion rate of exogenous glucose.

We calculated and defined organ-specific IR in the liver, skeletal muscle, and adipose tissue as described previously [27–30]. Hepatic IR indices were calculated as the product of fasting HGP and fasting plasma insulin (FPI) concentration (HGP×FPI [(mg·kg^{-1}·min^{-1})×(μU/mL)]) and suppression of HGP by insulin during a clamp study (%HGP). The skeletal muscle IR index was calculated as insulin-stimulated glucose disposal (Rd), and the adipose tissue IR index was calculated as suppression of FFA by insulin during a clamp study (%FFA).

Statistical Analysis

All analyses were performed using SPSS software version 21.0 (SPSS Inc., Chicago, IL, USA). All values are expressed as mean ± SEM, unless stated otherwise. The relationship between individual variables was assessed by Pearson's correlation for parametric variables and by Spearman's correlation for non-parametric variables. Multiple linear regression analysis was used to assess independent determinants of organ-specific IR. The differences between the two groups were assessed by Student's *t*-test for continuous variables and chi-square test for categorical variables. Data involving more than two groups were assessed by analysis of variance (ANOVA). Statistical significance was considered to be $P<0.05$.

Results

Organ-specific IR and Clinical Characteristics in Patients with NAFLD

The characteristics of the study subjects and their metabolic profiles are shown in Table 1. During the clamp study, plasma glucose concentrations were maintained at baseline values (103±1 mg/dL; mean ± SEM), and steady-state plasma insulin concentrations were reached at 110.2±3.6 μU/mL. Basal HGP was 2.09±0.08 mg·kg^{-1}·min^{-1} in subjects with normal glucose tolerance (NGT), 2.18±0.10 mg·kg^{-1}·min^{-1} in subjects with impaired glucose tolerance (IGT) and 2.67±0.12 mg·kg^{-1}·min^{-1} in subjects with T2DM. Rd was 3.81±0.18 mg·kg^{-1}·min^{-1} in NGT, 3.27±0.17 mg·kg^{-1}·min^{-1} in IGT and 3.57±0.14 mg·kg^{-1}·min^{-1} in T2DM. Basal FFA was 0.47±0.05 mEq/L in NGT, 0.56±0.04 mEq/L in IGT and 0.60±0.04 mEq/L in T2DM. Basal HGP showed a significant positive correlation with fasting plasma glucose levels ($r=0.48$, $P<0.001$). Rd showed a significant positive correlation with basal oxygen consumption rate per body weight (VO_2) ($r=0.42$, $P<0.01$). FFA and HGP were suppressed from baseline by 77.0±1.4% and 69.3±2.8%, respectively. These values are similar to previous data in Japanese [31] and European descent [1,27,29] subjects.

The relationship between clinical characteristics and organ-specific insulin sensitivity/resistance indices is shown in Table 2. HGP×FPI was significantly correlated with Rd ($r=-0.57$, $P<0.001$), %HGP with %FFA ($r=0.38$, $P<0.01$), and Rd with %FFA ($r=0.27$, $P<0.05$) suggesting that the IRs in the liver, skeletal muscle, and adipose tissue were significantly associated with each other, although the correlation was not very strong.

Ectopic Fat and Organ-specific IR

Histological liver steatosis score was strongly correlated with IHL measured by ^{1}H-MRS ($r=0.75$, $P<0.001$).

Liver steatosis score was significantly correlated with Rd ($r=-0.47$, $P<0.001$) as well as HGP×FPI ($r=0.43$, $P<0.001$) (Table 2). Similarly, IHL was significantly correlated with Rd ($r=-0.32$, $P<0.05$) and tended to be correlated with HGP×FPI ($r=0.25$, $P=0.09$) (Figure 1A, 1B). In the multiple regression analysis, liver steatosis score was significantly correlated with both HGP×FPI ($\beta=0.284$, $P<0.05$) and Rd ($\beta=-0.300$, $P<0.01$) after adjusting for age, sex, and BMI. Correlation of liver steatosis score with Rd ($\beta=-0.261$, $P<0.05$) was significant after further adjusting for total fat mass (Table 3). When stratified by steatosis score, HGP×FPI was significantly higher and Rd was significantly lower in the score 3 steatosis group compared to the score 0 steatosis group ($P<0.01$; $P<0.001$, respectively) (Figure 1C,1D).

Unexpectedly, indices of fat accumulation in the skeletal muscle (IMCL) and adipose tissue were not associated with their own organ-specific IR (Table 2). IMCL and fat-free mass were not correlated with Rd ($r=-0.16$, $P=0.26$; $r=-0.22$, $P=0.08$, respectively) (Figure 2A,2B). Total fat mass and its percentage were correlated with HGP×FPI ($r=0.50$, $P<0.001$; $r=0.48$, $P<0.001$, respectively) and Rd ($r=-0.59$, $P<0.001$; $r=-0.52$, $P<0.001$, respectively), but not with %FFA ($r=-0.21$, $P=0.10$; $r=-0.00$, $P=0.99$, respectively) (Figure 2C,2D).

Similar results were obtained when Rd was normalized by steady state plasma insulin (Rd/SSPI) (Table 2).

Because it may be possible that T2DM itself is associated with IR independently with organ steatosis, we analyzed the subjects with or without T2DM. Age, hemoglobin A1c, fasting plasma glucose, 2-h glucose level of 75-g OGTT and basal HGP were significantly higher in T2DM group compared to non-DM group (Table 1). Regardless of the presence or absence of T2DM, liver steatosis score was significantly correlated with Rd as well as HGP×FPI, and IMCL and total fat mass were not correlated with Rd or %FFA respectively (Table 4, Table 5). The results of the multiple regression analysis are shown in Table S1 and Table S2.

Discussion

We comprehensively and simultaneously evaluated ectopic fat accumulation and organ-specific IR in insulin-target organs in Japanese people with NAFLD, and found the following: 1) the IRs in the liver, skeletal muscle, and adipose tissue were associated with each other, 2) indices of fat accumulation in the skeletal muscle and adipose tissue were not associated with their own organ-specific IR, and 3) liver fat was associated with skeletal muscle IR as well as hepatic IR, independently of age, sex, BMI and total fat mass (Figure S1).

Although the IRs in the liver, skeletal muscle, and adipose tissue were associated with each other, the relation was relatively weak. There are a couple possible explanations for this result. First, the main site and the severity of IR may vary among organs and individuals [4]. Second, possibly the %HGP and %FFA are not

Table 1. Clinical characteristics of the study subjects.

	All	non-DM (NGT+IGT)	T2DM	*P* value*
n	69	32	37	
Age (years)	51±2	46±3	55±2	0.008[b]
Sex (Male/Female)	42/27	23/9	19/18	0.082
Body mass index (kg/m^2)	30.3±0.9	30.9±1.2	29.8±1.4	0.526
Weight (kg)	82.3±2.7	86.5±3.8	78.6±3.9	0.152
Fat-free mass (kg)	50.2±1.3	52.7±1.6	47.9±1.9	0.058
Total fat mass (kg)	30.6±2.0	31.0±2.9	30.2±2.9	0.855
Body fat percentage (%)	36.3±1.3	35.6±1.9	37.0±1.8	0.594
Historogical scores				
Steatosis (0/1/2/3)	5/33/15/16	4/13/5/10	1/20/10/6	
Grade (0/1/2/3)	15/35/16/3	10/14/7/1	5/21/9/2	
Stage (0/1/2/3/4)	20/29/6/11/3	12/14/1/4/1	8/15/5/7/2	
NAFLD activity score (0/1/2/3/4/5/6/7/8)	3/5/12/14/12/9/13/1/0	2/4/4/7/4/5/5/1/0	1/1/8/7/8/4/8/0/0	
IHL (mmol/L)	9.63±1.01	7.30±1.27	11.23±1.41	0.056
IMCL (AU, ratio relative to creatine)	28.29±1.49	27.91±2.21	28.58±2.04	0.827
Glucose tolerance (NGT/IGT/DM)	11/21/37			
Hemoglobin A1C (%)	6.5±0.1	6.0±0.1	7.0±0.1	<0.001[c]
Fasting plasma glucose (mg/dL)	111±2	100±2	121±3	<0.001[c]
2-h glucose (mg/dL)	208±10	142±6	265±12	<0.001[c]
Fasting plasma insulin (μU/mL)	14.0±1.0	15.1±1.5	13.1±1.3	0.318
2-h insulin (μU/mL)	139.1±12.6	157.2±21.8	123.5±13.7	0.182
Insulinogenic index [(μU/mL)/(mg/dL)]	0.72±0.09	0.95±0.16	0.52±0.09	0.019[a]
Fasting C-peptide (ng/mL)	2.9±0.1	3.1±0.2	2.7±0.2	0.199
Fasting FFAs (mEq/L)	0.57±0.03	0.53±0.03	0.60±0.04	0.254
Total cholesterol (mg/dL)	176±4	185±6	169±6	0.061
Triglycerides (mg/dL)	153±11	150±10	155±18	0.801
HDL cholesterol (mg/dL)	41±1	41±2	41±2	0.927
Aspartate aminotransferase (IU/L)	37±2	37±3	37±3	0.969
Alanine aminotransferase (IU/L)	60±4	62±6	59±5	0.752
Basal HGP (mg·kg^{-1}·min^{-1})	2.43±0.08	2.15±0.07	2.67±0.12	0.001[b]
HGP×FPI [(mg·kg^{-1}·min^{-1})×(μU/mL)]	32.0±2.0	31.2±2.8	32.7±2.9	0.707
Euglycemic hyperinsulinemic clamp [clamp period]				
Clamped glucose (mg/dL)	103±1	102±2	104±2	0.592
Steady state plasma insulin (μU/mL)	110.2±3.6	115.7±6.0	105.3±4.2	0.164
FFAs (mEq/L)	0.13±0.01	0.13±0.01	0.13±0.01	0.884
%FFA (%)	77.0±1.4	75.9±2.0	78.0±1.9	0.455
HGP (mg·kg^{-1}·min^{-1})	0.69±0.07	0.56±0.07	0.81±0.12	0.088
%HGP (%)	69.3±2.8	73.4±3.5	65.8±4.1	0.170
Rd (mg·kg^{-1}·min^{-1})	3.52±0.10	3.45±0.14	3.57±0.14	0.556
Rd/SSPI [(mg·kg^{-1}·min^{-1})/(μU/mL)]	0.035±0.002	0.033±0.003	0.037±0.003	0.332
VO_2 (ml·kg^{-1}·min^{-1})	2.85±0.04	2.84±0.07	2.86±0.06	0.817

Data are presented as n or mean ± SEM.
IHL, intrahepatic lipid; IMCL, intramyocellular lipid; AU, arbitrary units; HGP, hepatic glucose production; FPI, fasting plasma insulin; SSPI, steady state plasma insulin; VO_2, basal oxygen consumption rate per body weight.
*Difference between the non-DM group and the T2DM group.
[a]$P<0.05$,
[b]$P<0.01$,
[c]$P<0.001$.
doi:10.1371/journal.pone.0092170.t001

completely suitable for indices of hepatic and adipose tissue IR, respectively, and might not fully exhibit inter-individual variation because HGP and lipolysis appeared to be more sensitive to suppression by insulin compared to stimulation of Rd by insulin

Table 2. Univariate correlation between ectopic fat and organ-specific insulin resistance.

	HGP×FPI		%HGP		Rd		Rd/SSPI		%FFA	
	r	*P*	*r*	*P*	*r*	*P*	*r*	*P*	*r*	*P*
HGP×FPI	1	–	−0.130	0.288	−0.574[c]	<0.001	−0.489[c]	<0.001	−0.168	0.167
%HGP	−0.130	0.288	1	–	0.167	0.170	0.387[b]	0.001	0.375[b]	0.002
Rd	−0.574[c]	<0.001	0.167	0.170	1	–	0.766[c]	<0.001	0.272[a]	0.024
Rd/SSPI	−0.489[c]	<0.001	0.387[b]	0.001	0.766[c]	<0.001	1	–	0.296[a]	0.014
%FFA	−0.168	0.167	0.375[b]	0.002	0.272[a]	0.024	0.296[a]	0.014	1	–
Steatosis	0.428[c]	<0.001	−0.148	0.226	−0.473[c]	<0.001	−0.430[c]	<0.001	−0.121	0.322
Grade	0.338[b]	0.004	−0.111	0.362	−0.376[b]	0.001	−0.338[b]	0.005	−0.055	0.656
Stage	0.283[a]	0.019	−0.098	0.422	−0.348[b]	0.003	−0.261[a]	0.031	−0.010	0.933
IHL	0.245	0.089	−0.114	0.436	−0.315[a]	0.028	−0.271	0.062	−0.135	0.356
IMCL	0.250	0.065	−0.215	0.115	−0.156	0.256	−0.183	0.185	−0.060	0.662
Fat-free mass	0.031	0.801	−0.117	0.347	−0.216	0.079	−0.211	0.090	−0.433[c]	<0.001
Total fat mass	0.495[c]	<0.001	−0.147	0.235	−0.594[c]	<0.001	−0.536[c]	<0.001	−0.205	0.096
Body fat percentage	0.481[c]	<0.001	−0.115	0.355	−0.518[c]	<0.001	−0.478[c]	<0.001	−0.001	0.994
VO_2	−0.129	0.342	0.191	0.158	0.418[b]	0.001	0.405[b]	0.002	0.115	0.397

HGP, hepatic glucose production; FPI, fasting plasma insulin; SSPI, steady state plasma insulin; IHL, intrahepatic lipid; IMCL, intramyocellular lipid; VO_2, basal oxygen consumption rate per body weight.
[a]$P<0.05$,
[b]$P<0.01$,
[c]$P<0.001$.
doi:10.1371/journal.pone.0092170.t002

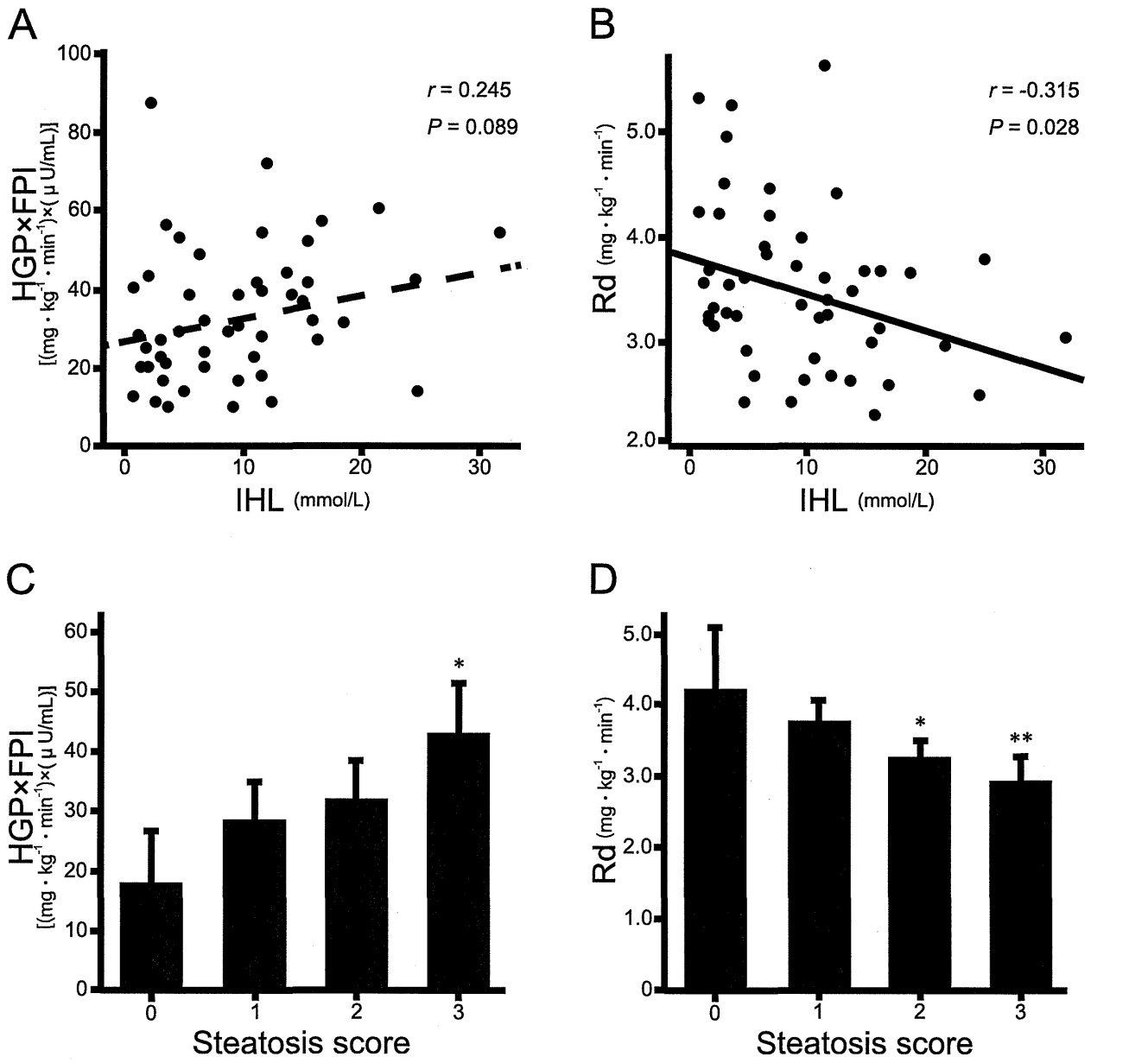

Figure 1. Correlation between liver fat and organ-specific insulin resistance (IR). (A) univariate correlation between IR in the liver (HGP×FPI) and liver fat (IHL) ($r = 0.25$, $P = 0.09$). (B) univariate correlation between skeletal muscle IR index (Rd) and liver fat (IHL) ($r = -0.32$, $P<0.05$). (C) IR in the liver (HGP×FPI) stratified by steatosis score. (D) skeletal muscle IR index (Rd) stratified by steatosis score. *$P<0.05$ vs. score 0 steatosis group. **$P<0.01$ vs. score 0 steatosis group.
doi:10.1371/journal.pone.0092170.g001

Table 3. Multiple regression models predicting HGP×FPI and Rd.

	HGP×FPI		Rd	
	β	*P*	β	*P*
Steatosis (Model 1)	0.284	0.026[a]	−0.300	0.007[b]
Steatosis (Model 2)	0.216	0.098	−0.261	0.027[a]

HGP, hepatic glucose production; FPI, fasting plasma insulin.
Model 1, adjusted for, age, sex, and body mass index; Model 2, adjusted for, age, sex, body mass index, and total fat mass.
[a]$P<0.05$,
[b]$P<0.01$.
doi:10.1371/journal.pone.0092170.t003

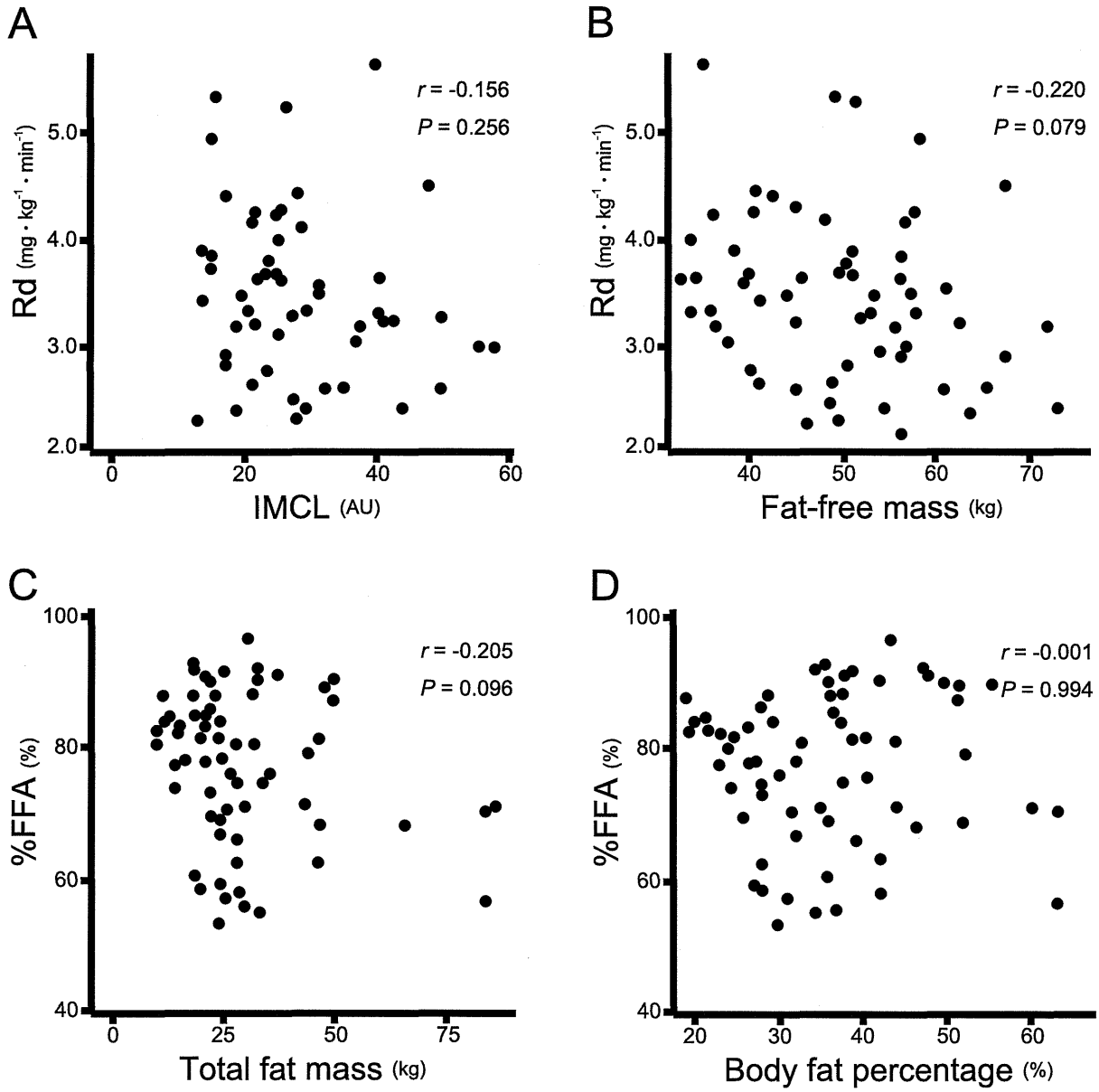

Figure 2. Correlation between ectopic fat and organ-specific insulin resistance (IR). (A) univariate correlation between skeletal muscle IR index (Rd) and intramyocellular lipid (IMCL) ($r = -0.16$, $P = 0.26$). (B) univariate correlation between Rd and fat-free mass ($r = 0.22$, $P = 0.08$). (C) univariate correlation between adipose tissue IR index (%FFA) and total fat mass ($r = -0.21$, $P = 0.10$). (D) univariate correlation between %FFA and body fat percentage ($r = -0.00$, $P = 0.99$).
doi:10.1371/journal.pone.0092170.g002

[32,33]. Lowering steady-state insulin levels by a reduced insulin infusion rate might improve the specificity of these indices to reflect organ insulin sensitivity.

In the present study, IMCL was not associated with skeletal muscle IR. The participants in this study had a wide BMI range (21.3–54.9 kg/m^2) and subjects may have different physical exercise habits with various intensities. IMCL is increased not only by obesity but also by enhanced physical fitness [34]. Therefore, absolute fat contents do not always predict IR in the skeletal muscle, thus, toxic lipids that cause IR in the skeletal muscle should be further researched. Similarly, we failed to find any relationship between fat mass or its percentage and adipose tissue IR. Although we evaluated only total fat mass, distribution of adipose tissue may potentially determine insulin action. Indeed, visceral fat, but not subcutaneous fat, is reported to be associated with %FFA [35]. Therefore, future studies should evaluate visceral and subcutaneous fat masses separately and evaluate the relation to %FFA in Japanese people.

In addition to the previously well-recognized relationship between adipose tissue mass and IR in the liver and skeletal muscle [36], the present study showed a distinct relationship between liver fat and skeletal muscle IR independently of age, sex, and BMI. Although our results are consistent with previous studies showing that liver fat plays an important role in peripheral IR as well as hepatic IR [14,15], not all associations among components of ectopic fat and organ-specific IR were examined simultaneously in these studies. Our findings suggest that hepatic steatosis *per se* is a central surrogate pathology indicative of IR in both liver and

Table 4. Univariate correlation between ectopic fat and organ-specific insulin resistance in subjects without type 2 diabetes ($n = 32$).

	HGP×FPI		%HGP		Rd		Rd/SSPI		%FFA	
	r	*P*	*r*	*P*	*r*	*P*	*r*	*P*	*r*	*P*
HGP×FPI	1	–	−0.132	0.470	−0.551[b]	0.001	−0.554[b]	0.001	−0.095	0.607
%HGP	−0.132	0.470	1	–	0.101	0.583	0.121	0.509	0.370[a]	0.037
Rd	−0.551[b]	0.001	0.101	0.583	1	–	0.798[c]	<0.001	0.297	0.099
Rd/SSPI	−0.554[b]	0.001	0.121	0.509	0.798[c]	<0.001	1	–	0.210	0.250
%FFA	−0.095	0.607	0.370[a]	0.037	0.297	0.099	0.210	0.250	1	–
Steatosis	0.524[b]	0.002	−0.008	0.964	−0.478[b]	0.006	−0.409[a]	0.020	0.099	0.589
Grade	0.403[a]	0.022	−0.115	0.530	−0.487[b]	0.005	−0.497[b]	0.004	0.172	0.348
Stage	0.206	0.258	−0.033	0.859	−0.305	0.090	−0.194	0.286	0.114	0.534
IHL	0.198	0.403	0.155	0.515	−0.570[b]	0.009	−0.414	0.070	−0.173	0.465
IMCL	0.318	0.130	−0.334	0.110	−0.128	0.552	−0.151	0.480	−0.172	0.421
Fat-free mass	−0.017	0.926	−0.262	0.154	−0.050	0.788	−0.118	0.527	−0.321	0.078
Total fat mass	0.523[b]	0.003	0.030	0.873	−0.728[c]	<0.001	−0.586[b]	0.001	−0.082	0.660
Body fat percentage	0.488[b]	0.005	0.056	0.763	−0.729[c]	<0.001	−0.599[c]	<0.001	0.045	0.811
VO_2	−0.045	0.829	0.131	0.523	0.379	0.057	0.356	0.074	0.009	0.964

HGP, hepatic glucose production; FPI, fasting plasma insulin; SSPI, steady state plasma insulin; IHL, intrahepatic lipid; IMCL, intramyocellular lipid; VO_2, basal oxygen consumption rate per body weight.
[a]$P<0.05$,
[b]$P<0.01$,
[c]$P<0.001$.
doi:10.1371/journal.pone.0092170.t004

Table 5. Univariate correlation between ectopic fat and organ-specific insulin resistance in subjects with type 2 diabetes ($n = 37$).

	HGP×FPI		%HGP		Rd		Rd/SSPI		%FFA	
	r	*P*	*r*	*P*	*r*	*P*	*r*	*P*	*r*	*P*
HGP×FPI	1	–	−0.119	0.483	−0.600[c]	<0.001	−0.461[b]	0.005	−0.234	0.164
%HGP	−0.119	0.483	1	–	0.233	0.165	0.582[c]	<0.001	0.419[a]	0.010
Rd	−0.600[c]	<0.001	0.233	0.165	1	–	0.746[c]	<0.001	0.244	0.145
Rd/SSPI	−0.461[b]	0.005	0.582[c]	<0.001	0.746[c]	<0.001	1	–	0.346[a]	0.039
%FFA	−0.234	0.164	0.419[a]	0.010	0.244	0.145	0.346[a]	0.039	1	–
Steatosis	0.390[a]	0.017	−0.306	0.066	−0.459[b]	0.004	−0.486[b]	0.003	−0.340[a]	0.039
Grade	0.263	0.115	−0.023	0.894	−0.282	0.091	−0.216	0.206	−0.304	0.067
Stage	0.357[a]	0.030	−0.096	0.571	−0.478[b]	0.003	−0.473[b]	0.004	−0.168	0.320
IHL	0.286	0.133	−0.122	0.529	−0.209	0.277	−0.219	0.262	−0.197	0.306
IMCL	0.202	0.276	−0.128	0.491	−0.178	0.338	−0.220	0.243	0.025	0.893
Fat-free mass	0.084	0.626	−0.136	0.430	−0.314	0.062	−0.276	0.108	−0.508[b]	0.002
Total fat mass	0.478[b]	0.003	−0.301	0.074	−0.493[b]	0.002	−0.497[b]	0.002	−0.305	0.071
Body fat percentage	0.473[b]	0.004	−0.227	0.183	−0.362[a]	0.030	−0.374[a]	0.027	−0.049	0.775
VO_2	−0.211	0.264	0.264	0.159	0.460[a]	0.011	0.460[a]	0.012	0.212	0.261

HGP, hepatic glucose production; FPI, fasting plasma insulin; SSPI, steady state plasma insulin; IHL, intrahepatic lipid; IMCL, intramyocellular lipid; VO_2, basal oxygen consumption rate per body weight.
[a]$P<0.05$,
[b]$P<0.01$,
[c]$P<0.001$.
doi:10.1371/journal.pone.0092170.t005

skeletal muscle in patients with NAFLD. In addition, there may be a network between the liver and skeletal muscle to maintain whole body energy homeostasis. Accordingly, whether hepatic steatosis is a consequence or cause of skeletal muscle IR remains uncertain because a longitudinal observation of the relationship is lacking. One hypothesis is that skeletal muscle IR causes obesity and subsequent hepatic steatosis as experimentally shown in mice with muscle-selective IR [37]. Indeed, Flannery et al. recently reported that skeletal muscle IR promotes increased hepatic *de novo* lipogenesis and hepatic steatosis in the elderly [38]. A second hypothesis is the neuronal pathway from the liver might modulate peripheral insulin sensitivity [11]. A third hypothesis is that some nutrients, such as fatty acids and amino acids, might link hepatic steatosis and skeletal muscle IR [39]. A fourth hypothesis is that a liver-derived hormone (a hepatokine) affects the distant organ insulin sensitivity. We previously isolated hepatokine selenoprotein P, which is overproduced under an overnutrition state and causes IR both in the liver and skeletal muscle [13]. In addition, serum levels of selenoprotein P are inversely associated with serum levels of adiponectin [40] that enhance skeletal muscle insulin sensitivity [12]. Therefore, overproduction of selenoprotein P in association with hepatic steatosis, by directly or indirectly lowering adiponectin levels, causes skeletal muscle IR.

There are several limitations to this study. First, this was an observational study, and we were unable to examine causal associations. A large-scale longitudinal study is needed to clarify whether hepatic steatosis is a consequence or cause of skeletal muscle IR. Second, many of the study subjects had glucose intolerance/diabetes, although the severity was relatively mild as shown by the OGTT. Therefore, IR of each organ was possibly greater in our study subjects than in the general population, which could have influenced the results. Third, fifteen out of 69 subjects were taking metformin which might influence hepatic glucose production. However, major study results were similar in diabetic subjects, non-diabetic subjects, and subjects without metformin (data not shown). Fourth, we did not collect arterial or arterialized blood samples to perform the insulin clamp because these were not included in the manufacturer's protocol of the artificial pancreas model STG-55. Further study should be required to confirm our conclusion by using arterial or arterialized blood samples.

In summary, the present study revealed an unexpected lack of an association between fat and local organ-specific IR in the skeletal muscle and adipose tissue. Instead, liver fat is strongly associated with skeletal muscle IR as well as with liver IR, suggesting a central role of fatty liver in the development of IR and that a network exists between liver and skeletal muscle to maintain whole-body energy homeostasis.

Supporting Information

Figure S1 Correlation between ectopic fat and insulin resistance (IR) in the liver, skeletal muscle, and adipose tissue. Liver fat (steatosis score) was associated with skeletal muscle IR index (Rd) as well as with IR in the liver (HGP×FPI). Intramyocellular lipid was not associated with skeletal muscle IR index (Rd). Total fat mass was associated with HGP×FPI and Rd, but not with adipose tissue IR index (%FFA).
(PDF)

Table S1 Multiple regression models predicting HGP×FPI and Rd in subjects without type 2 diabetes ($n = 32$). HGP, hepatic glucose production; FPI, fasting plasma insulin Model 1, adjusted for, age, sex, and body mass index; Model 2, adjusted for, age, sex, body mass index, and total fat mass.
(DOC)

Table S2 Multiple regression models predicting HGP×FPI and Rd in subjects with type 2 diabetes ($n = 37$). HGP, hepatic glucose production; FPI, fasting plasma insulin Model 1, adjusted for, age, sex, and body mass index; Model 2, adjusted for, age, sex, body mass index, and total fat mass.
(DOC)

Acknowledgments

We thank Dr. Tatsuya Yamashita (Kanazawa University) and Dr. Kuniaki Arai (Kanazawa University) for performing the liver biopsies and Mr. Kaito Iwayama (University of Tsukuba) for analyzing glucose turnover.

Author Contributions

Conceived and designed the experiments: TT. Performed the experiments: KK TT YT HM TO. Analyzed the data: KK TT. Contributed reagents/materials/analysis tools: YR KT. Wrote the paper: KK TT. Contributed to discussion and reviewed the manuscript: SN MM OM SK.

References

1. Marchesini G, Brizi M, Bianchi G, Tomassetti S, Bugianesi E, et al. (2001) Nonalcoholic fatty liver disease: a feature of the metabolic syndrome. Diabetes 50: 1844–1850.
2. Chalasani N, Younossi Z, Lavine JE, Diehl AM, Brunt EM, et al. (2012) The diagnosis and management of non-alcoholic fatty liver disease: practice Guideline by the American Association for the Study of Liver Diseases, American College of Gastroenterology, and the American Gastroenterological Association. Hepatology 55: 2005–2023.
3. Takamura T, Misu H, Ota T, Kaneko S (2012) Fatty liver as a consequence and cause of insulin resistance: Lessons from type 2 diabetic liver. Endocr J 59: 745–763.
4. Matsuda M, DeFronzo RA (1999) Insulin sensitivity indices obtained from oral glucose tolerance testing: comparison with the euglycemic insulin clamp. Diabetes Care 22: 1462–1470.
5. Matsuzawa N, Takamura T, Kurita S, Misu H, Ota T, et al. (2007) Lipid-induced oxidative stress causes steatohepatitis in mice fed an atherogenic diet. Hepatology 46: 1392–1403.
6. Nakamura S, Takamura T, Matsuzawa-Nagata N, Takayama H, Misu H, et al (2009) Palmitate induces insulin resistance in H4IIEC3 hepatocytes through reactive oxygen species produced by mitochondria. J Biol Chem 284: 14809–14818.
7. Jornayvaz FR, Shulman GI (2012) Diacylglycerol activation of protein kinase Cε and hepatic insulin resistance. Cell Metab 15: 574–584.
8. Mootha VK, Lindgren CM, Eriksson KF, Subramanian A, Sihag S, et al. (2003) PGC-1alpha-responsive genes involved in oxidative phosphorylation are coordinately downregulated in human diabetes. Nat Genet 34: 267–273.
9. Takamura T, Misu H, Matsuzawa-Nagata N, Sakurai M, Ota T, et al. (2008) Obesity upregulates genes involved in oxidative phosphorylation in livers of diabetic patients. Obesity 16: 2601–2609.
10. Sakurai M, Takamura T, Ota T, Ando H, Akahori H, et al. (2007) Liver steatosis, but not fibrosis, is associated with insulin resistance in nonalcoholic fatty liver disease. J Gastroenterol 42: 312–317.
11. Uno K, Katagiri H, Yamada T, Ishigaki Y, Ogihara T, et al. (2006) Neuronal pathway from the liver modulates energy expenditure and systemic insulin sensitivity. Science 312: 1656–1659.
12. Iwabu M, Yamauchi T, Okada-Iwabu M, Sato K, Nakagawa T, et al. (2010) Adiponectin and AdipoR1 regulate PGC-1alpha and mitochondria by Ca(2+) and AMPK/SIRT1. Nature 464: 1313–1319.
13. Misu H, Takamura T, Takayama H, Hayashi H, Matsuzawa-Nagata N, et al. (2010) A liver-derived secretory protein, selenoprotein P, causes insulin resistance. Cell Metab 12: 483–495.
14. Kotronen A, Seppälä-Lindroos A, Bergholm R, Yki-Järvinen H (2008) Tissue specificity of insulin resistance in humans: fat in the liver rather than muscle is associated with features of the metabolic syndrome. Diabetologia 51: 130–138.
15. D'Adamo E, Cali AM, Weiss R, Santoro N, Pierpont B, et al. (2010) Central role of fatty liver in the pathogenesis of insulin resistance in obese adolescents. Diabetes Care 33: 1817–1822.

16. McPherson S, Jonsson JR, Cowin GJ, O'Rourke P, Clouston AD, et al. (2009) Magnetic resonance imaging and spectroscopy accurately estimate the severity of steatosis provided the stage of fibrosis is considered. J Hepatol 51: 389–397.
17. American Diabetes Association (2010) Standards of medical care in diabetes–2010. Diabetes Care 33: S11–S61.
18. DeFronzo RA, Tobin JD, Andres R (1979) Glucose clamp technique: a method for quantifying insulin secretion and resistance. Am J Physiol 237: E214–E223.
19. Finegood DT, Bergman RN, Vranic M (1987) Estimation of endogenous glucose production during hyperinsulinemic-euglycemic glucose clamps. Diabetes 36: 914–924.
20. Kleiner DE, Brunt EM, Van Natta M, Behling C, Contos MJ, et al; Nonalcoholic Steatohepatitis Clinical Research Network (2005) Design and validation of a histological scoring system for nonalcoholic fatty liver disease. Hepatology 41: 1313–1321.
21. Brunt EM, Janney CG, Di Bisceglie AM, Neuschwander-Tetri BA, Bacon BR (1999) Nonalcoholic steatohepatitis: a proposal for grading and staging the histological lesions. Am J Gastroenterol 9: 2467–2474.
22. Ryysy L, Häkkinen AM, Goto T, Vehkavaara S, Westerbacka J, et al. (2000) Hepatic fat content and insulin action on free fatty acids and glucose metabolism rather than insulin absorption are associated with insulin requirements during insulin therapy in type 2 diabetic patients. Diabetes 49: 749–758.
23. Szczepaniak LS, Babcock EE, Schick F, Dobbins RL, Garg A, et al. (1999) Measurement of intracellular triglyceride stores by H spectroscopy: validation in vivo. Am J Physiol 276: E977–E989.
24. Wolfe R (1992) Radioactive and Stable-Isotope Tracers in Biomedicine: Principles and Practice of Kinetic Analysis. New York, Wiley–Liss.
25. Cobelli C, Toffolo G, Bier DM, Nosadini R (1987) Models to interpret kinetic data in stable isotope tracer studies. Am J Physiol 253: E551–E564.
26. Cobelli C, Mari A, Ferrannini E (1987) Non-steady state: error analysis of Steele's model and developments for glucose kinetics. Am J Physiol 252: E679–E689.
27. Lomonaco R, Ortiz-Lopez C, Orsak B, Finch J, Webb A, et al. (2011) Role of ethnicity in overweight and obese patients with nonalcoholic steatohepatitis. Hepatology 54: 837–845.
28. Abdul-Ghani MA, Matsuda M, Balas B, DeFronzo RA (2007) Muscle and liver insulin resistance indexes derived from the oral glucose tolerance test. Diabetes Care 30: 89–94.
29. Gastaldelli A, Cusi K, Pettiti M, Hardies J, Miyazaki Y, et al. (2007) Relationship between hepatic/visceral fat and hepatic insulin resistance in nondiabetic and type 2 diabetic subjects. Gastroenterology 133: 496–506.
30. Kashyap S, Belfort R, Gastaldelli A, Pratipanawatr T, Berria R, et al. (2003) A sustained increase in plasma free fatty acids impairs insulin secretion in nondiabetic subjects genetically predisposed to develop type 2 diabetes. Diabetes 52: 2461–2474.
31. Nagasaka S, Tokuyama K, Kusaka I, Hayashi H, Rokkaku K, et al. (1999) Endogenous glucose production and glucose effectiveness in type 2 diabetic subjects derived from stable-labeled minimal model approach. Diabetes 48: 1054–1060.
32. Yki-Järvinen H, Young AA, Lamkin C, Foley JE (1987) Kinetics of glucose disposal in whole body and across the forearm in man. J Clin Invest 79: 1713–1719.
33. Bugianesi E, Gastaldelli A, Vanni E, Gambino R, Cassader M, et al. (2005) Insulin resistance in non-diabetic patients with non-alcoholic fatty liver disease: sites and mechanisms. Diabetologia 48: 634–642.
34. Thamer C, Machann J, Bachmann O, Haap M, Dahl D, et al. (2003) Intramyocellular lipids: anthropometric determinants and relationships with maximal aerobic capacity and insulin sensitivity. J Clin Endocrinol Metab 88: 1785–1791.
35. Kurioka S, Murakami Y, Nishiki M, Sohmiya M, Koshimura K, et al. (2002) Relationship between visceral fat accumulation and anti-lipolytic action of insulin in patients with type 2 diabetes mellitus. Endocr J 49: 459–464.
36. Iozzo P (2009) Viewpoints on the way to a consensus session: where does insulin resistance start? The adipose tissue. Diabetes Care (Suppl. 2): S168–S173.
37. Kim JK, Michael MD, Previs SF, Peroni OD, Mauvais-Jarvis F, et al. (2000) Redistribution of substrates to adipose tissue promotes obesity in mice with selective insulin resistance in muscle. J Clin Invest 105: 1791–1797.
38. Flannery C, Dufour S, Rabol R, Shulman GI, Petersen KF (2012) Skeletal muscle insulin resistance promotes increased hepatic de novo lipogenesis, hyperlipidemia, and hepatic steatosis in the elderly. Diabetes 61: 2711–2717.
39. Newgard CB (2012) Interplay between lipids and branched-chain amino acids in development of insulin resistance. Cell Metab 15: 606–614.
40. Misu H, Ishikura K, Kurita S, Takeshita Y, Ota T, et al. (2012) Inverse correlation between serum levels of selenoprotein P and adiponectin in patients with type 2 diabetes. PLoS One 7: e34952. doi: 10.1371/journal.pone.0034952. Epub 2012 April 4.

Cancer Immunol Immunother (2014) 63:479–489
DOI 10.1007/s00262-014-1529-8

ORIGINAL ARTICLE

P53, hTERT, WT-1, and VEGFR2 are the most suitable targets for cancer vaccine therapy in HLA-A24 positive pancreatic adenocarcinoma

Takeshi Terashima · Eishiro Mizukoshi · Kuniaki Arai · Tatsuya Yamashita · Mariko Yoshida · Hajime Ota · Ichiro Onishi · Masato Kayahara · Koushiro Ohtsubo · Takashi Kagaya · Masao Honda · Shuichi Kaneko

Received: 23 May 2013 / Accepted: 22 February 2014 / Published online: 16 March 2014

Abstract Cancer vaccine therapy is one of the most attractive therapies as a new treatment procedure for pancreatic adenocarcinoma. Recent technical advances have enabled the identification of cytotoxic T lymphocyte (CTL) epitopes in various tumor-associated antigens (TAAs). However, little is known about which TAA and its epitope are the most immunogenic and useful for a cancer vaccine for pancreatic adenocarcinoma. We examined the expression of 17 kinds of TAA in 9 pancreatic cancer cell lines and 12 pancreatic cancer tissues. CTL responses to 23 epitopes derived from these TAAs were analyzed using enzyme-linked immunospot (ELISPOT), CTL, and tetramer assays in 41 patients, and factors affecting the immune responses were investigated. All TAAs were frequently expressed in pancreatic adenocarcinoma cells, except for adenocarcinoma antigens recognized by T cells 1, melanoma-associated antigen (MAGE)-A1, and MAGE-A3. Among the epitopes recognized by CTLs in more than two patients in the ELISPOT assay, 6 epitopes derived from 5 TAAs, namely, MAGE-A3, p53, human telomerase reverse transcriptase (hTERT), Wilms tumor (WT)-1, and vascular endothelial growth factor receptor (VEGFR)2, could induce specific CTLs that showed cytotoxicity against pancreatic cancer cell lines. The frequency of lymphocyte subsets correlated well with TAA-specific immune response. Overall survival was significantly longer in patients with TAA-specific CTL responses than in those without. P53, hTERT, WT-1, and VEGFR2 were shown to be attractive targets for immunotherapy in patients with pancreatic adenocarcinoma, and the induction of TAA-specific CTLs may improve the prognosis of these patients.

Keywords Epitope · Immunotherapy · Cytotoxic T lymphocyte (CTL) · Enzyme-linked immunospot (ELISPOT)

Abbreviations

CTL	Cytotoxic T lymphocyte
TAA	Tumor-associated antigen
ELISPOT	Enzyme-linked immunospot
MAGE	Melanoma-associated antigen
hTERT	Human telomerase reverse transcriptase
WT-1	Wilms tumor-1
VEGFR	Vascular endothelial growth factor receptor
PBMC	Peripheral blood mononuclear cells
PCR	Polymerase chain reaction

Electronic supplementary material The online version of this article (doi:10.1007/s00262-014-1529-8) contains supplementary material, which is available to authorized users.

T. Terashima (✉) · E. Mizukoshi · K. Arai · T. Yamashita · T. Kagaya · M. Honda · S. Kaneko
Department of Gastroenterology, Graduate School of Medicine, Kanazawa University, 13-1 Takara-Machi, Kanazawa 920-8641, Ishikawa, Japan
e-mail: tera@m-kanazawa.jp

S. Kaneko
e-mail: skaneko@m-kanazawa.jp

M. Yoshida · H. Ota
Department of Gastroenterology, National Hospital Organization Kanazawa Medical Center, Kanazawa 920-8650, Ishikawa, Japan

I. Onishi · M. Kayahara
Department of Surgery, National Hospital Organization Kanazawa Medical Center, Kanazawa 920-8650, Ishikawa, Japan

K. Ohtsubo
Division of Medical Oncology, Cancer Research Institute, Kanazawa University, Kanazawa 920-0934, Ishikawa, Japan

Introduction

Pancreatic adenocarcinoma is the fourth leading cause of cancer death worldwide [1]. Despite recent advances in diagnostic techniques, pancreatic adenocarcinoma is diagnosed at an advanced stage in most patients and, consequently, the overall 5-year survival rate is <5 % [2]. Thus, the development of a new treatment option is needed to improve the prognosis of pancreatic cancer patients without toxicity.

Immunotherapy is one of the most attractive therapies as a new treatment procedure for melanoma and other solid tumors [3]. Recent technical advances have enabled the identification of various tumor-associated antigens (TAAs) [4–21]; however, few of their epitopes are inducers of cytotoxic T lymphocyte (CTL) responses against tumors [22]. Several kinds of epitope have also been identified in patients with pancreatic adenocarcinoma [23, 24]. However, previous studies focused on the identification and evaluation of a particular antigen, and different TAAs have not yet been compared simultaneously; therefore, little is known about which epitope is the most immunogenic and useful in eliciting clinical responses in pancreatic adenocarcinoma patients.

In the present study, we compared CTL responses with various TAA-derived epitopes in identical patients with pancreatic adenocarcinomas and examined the factors that affect immune responses. This approach provided information that is useful for selecting immunogenic TAAs and suitable patients and developing a new immunotherapy for pancreatic adenocarcinoma.

Materials and methods

Patients and clinical information

In this study, we examined 41 HLA-A24-positive patients with pancreatic adenocarcinoma and 14 healthy volunteers who were HLA-A24-positive, but did not have any cancers, as negative controls. Fine-needle biopsy, a surgical specimen, or autopsy was used for the pathological diagnosis of pancreatic adenocarcinoma in 18 patients. Diagnosis of the remaining 23 patients was achieved using the radiological findings of computed tomography and/or magnetic resonance imaging. We investigated patient background, treatment procedures, and outcomes.

Clinical information was obtained from the medical records of patients. We evaluated the tumor stage using TNM staging of the Union Internationale Contre Le Cancer (UICC) system (7th version) (UICC stage). The frequency of lymphocyte subsets was calculated by dividing the absolute lymphocyte count by the absolute leukocyte count. HLA typing of peripheral blood mononuclear cells (PBMCs) from patients and healthy volunteers was performed by the reverse sequence-specific oligonucleotide with polymerase chain reaction (PCR-RSSO). This study was approved by the Ethics Committees of Kanazawa University (No. 1237) and Kanazawa Medical Center (No. 17), and all patients gave written informed consent to participate in accordance with the Helsinki Declaration.

Table 1 Peptides used in this study

Peptide No.	TAA	Amino acid sequence	Reference
1	$ART1_{188}$	EYCLKFTKL	[14]
2	$ART4_{161}$	AFLRHAAL	[11]
3	$ART4_{899}$	DYPSLSATDI	[11]
4	Cyp-B_{109}	KFHRVIKDF	[7]
5	Cyp-B_{315}	DFMIQGGDF	[7]
6	Lck_{208}	HYTNASDGL	[8]
7	Lck_{488}	DYLRSVLEDF	[8]
8	MAGE-$A1_{135}$	NYKHCFPEI	[6]
9	MAGE-$A3_{195}$	IMPKAGLLI	[16]
10	$SART1_{690}$	EYRGFTQDF	[12]
11	$SART2_{899}$	SYTRLFLIL	[13]
12	$SART3_{109}$	VYDYNCHVDL	[21]
13	Her-2/neu_8	RWGLLLALL	[17]
14	$p53_{161}$	AIYKQSQHM	[18]
15	$p53_{204}$	EYLDDRNTF	[5]
16	$MRP3_{765}$	VYSDADIFL	[20]
17	$MRP3_{503}$	LYAWEPSFL	[20]
18	$hTERT_{461}$	VYGFVRACL	[4]
19	$hTERT_{324}$	VYAETKHFL	[4]
20	WT-1_{235}	CMTWNQMNL	[15]
21	$VEGFR2_{169}$	RFVPDGNRI	[19]
22	$VEGFR1_{1084}$	SYGVLLWEI	[10]
23	survivin$2B_{80}$	AYACNTSTL	[9]
24	HIV env_{584}	RYLRDQQLL	[25]
25	CMV $pp65_{328}$	QYDPVAALF	[26]

Synthetic peptides and preparation of PBMCs

The 23 epitopes derived from 17 different TAAs used in the present study are listed in Table 1. We selected epitopes that had previously been identified as HLA-A24-restricted and suggested to have immunogenicity in various cancers not restricted to pancreatic cancer [4–21]. Epitopes derived from the HIV envelope protein (HIV env_{584}) [25] and cytomegalovirus (CMV) pp65 (CMV$pp65_{328}$) [26] were also used to assess T cell responses. Peptides were synthesized at Mimotope (Melbourne, Australia), Sumitomo Pharmaceuticals (Osaka, Japan), COSMO BIO Co. (Tokyo, Japan), and Scrum Inc. (Tokyo, Japan). Purities were determined to be >80 % by analytical high-performance

liquid chromatography (HPLC). PBMCs were separated as described below; heparinized venous blood was diluted in phosphate-buffered saline (PBS) and loaded on Ficoll-Histopaque (Sigma, St. Louis, MO) in 50-ml tubes. After centrifugation at 2,000 rpm for 20 min at room temperature, PBMCs were harvested from the interphase, resuspended in PBS, centrifuged at 1,400 rpm for 10 min, and finally resuspended in complete culture medium consisting of RPMI (GibcoBRL, Grand Island, NY), 10 % heat-inactivated FCS (Gibco BRL), 100 U/ml penicillin, and 100 μg/ml streptomycin (Gibco BRL).

Cell lines

The HLA-A*2402 gene-transfected C1R cell line (C1R-A24) was cultured in RPMI 1640 medium containing 10 % FCS and 500 μg/ml hygromycin B (Sigma, St. Louis, MO), and K562 was cultured in RPMI 1640 medium containing 10 % FCS [27]. MiaPaca2, AsPC1, BxPC3, Panc-1, CAPAN1, and CAPAN2 were purchased from the American Type Culture Collection (VA, USA). YPK-1 and YPK-2 were kind gifts from Prof. Oka and Dr. Yoshimura (Yamaguchi University Graduate School of Medicine, Yamaguchi, Japan). PK-1 was provided by the RIKEN BRC through the National Bio-Resource Project of MEXT, Japan. Human pancreatic cancer cell lines were cultured in DMEM (GibcoBRL) or RPMI 1640 medium containing 10 % fetal calf serum (FCS). All media contained 100 U/mL penicillin and 100 μg/mL streptomycin.

RNA preparation and real-time PCR

The expression of TAA messenger RNA (mRNA) in human pancreatic cancer cell lines and pancreatic adenocarcinoma tissues was analyzed by real-time polymerase chain reaction (PCR). Cell lines were harvested, centrifuged, and washed with PBS, and total RNA was then isolated using Quick-Gene (Fuji Film, Tokyo). Total RNA from frozen pancreatic adenocarcinoma samples was isolated using a GenElute Mammalian Total RNA Miniprep Kit (Sigma-Aldrich) according to the manufacturer's protocol. cDNA was synthesized from 150 ng of total RNA using a high-capacity cDNA reverse transcription kit (PE Applied Biosystems, CA, USA) and was then mixed with TaqMan Universal Master Mix (PE Applied Biosystems) and each TaqMan probe. Primer pairs and probes for various TAAs and β-actin were obtained from the TaqMan assay reagents library. Thermal cycling conditions were 25 °C for 10 min, 37 °C for 120 min, and 85 °C for 1 min. cDNA was subjected to quantitative real-time PCR analyses targeting various TAAs and β-actin. Analyses were performed using the StepOne Real-Time PCR system and StepOne v2.0 software. Relative gene expression values were determined. Data are presented as fold differences in TAA expression normalized to the housekeeping gene β-actin as an endogenous reference.

Enzyme-linked immunospot assay (ELISPOT assay)

Ninety-six-well plates (Millititer, Millipore, Bedford, MA) were coated with anti-human interferon-γ (IFN-γ) (Mabtech, Nacka, Sweden) at 4 °C overnight and then washed 4 times with sterile PBS. The plates were then blocked with RPMI 1640 medium containing 5 % FCS for 2 h at room temperature. A total of 300,000 unfractionated PBMCs were added in duplicate cultures of RPMI 1640 containing 5 % FCS together with the peptides at 10 μg/ml. After 24 h, the plates were washed 8 times with PBS and incubated overnight with 100 μl of the biotin-conjugated anti-human IFN-γ antibody. After another 4 washes with PBS, streptavidin-AP was added for 2 h. Finally, the plates were washed again 4 times with PBS and developed with freshly prepared NBT/BCIP solution (Biorad, Hercules, CA). The reaction was stopped by washing with distilled water and drying at room temperature. Colored spots with fuzzy borders, which indicated the presence of IFN-γ-secreting cells, were counted. The number of specific spots was determined by subtracting the number of spots in the absence of the antigen. Responses were considered positive if 10 or more specific spots were detected and if the number of spots in the presence of an antigen was at least two-fold than that in its absence.

Peptide-specific CTL induction and cytotoxicity assay

Synthetic peptide-specific T cells were expanded from PBMCs in 96-well round-bottom plates (NUNC, Naperville, IL). Four hundred thousand cells/well were stimulated with synthetic peptides at 10 μg/ml, 10 ng/ml rIL-7, and 100 pg/ml rIL-12 (Sigma) in RPMI 1640 supplemented with 10 % heat-inactivated human AB serum, 100 U/ml penicillin, and 100 μg/ml streptomycin. The cultures were restimulated with 10 μg/ml peptide, 20 U/ml rIL-2 (Sigma), and 10^5 mitomycin C-treated autologous PBMCs as feeder cells on days 7 and 14. One hundred microliters of RPMI medium with 10 % human Ab serum and rIL-2 at a final concentration of 10 U/ml were added to each well on days 4, 11, and 18. The cytotoxicity assay was conducted on day 22.

The C1R-A24 and human pancreatic cancer cell lines were used as target cells for the ^{51}Cr release assay. C1R-A24 cells were incubated overnight with 10 μg/ml synthetic peptides and labeled with 25 μCi of ^{51}Cr for 1 h. Pancreatic cancer cell lines were also labeled with 25 μCi of ^{51}Cr for 1 h without incubation with peptides. After three washes with PBS, target cells were plated at 3,000 cells/well in complete medium

in round-bottom 96-well plates. Unlabeled K562 (120,000 cells/well) was added to reduce non-specific lysis. Peptide-stimulated PBMCs were added at various effector-to-target ratios as indicated. Maximum release was determined by the lysis of ^{51}Cr-labeled targets with 5 % Triton X-100 (Sigma Chemical). Spontaneous release was <10 % of maximum release for all experiments, except for when it was <15 % when the target cells were human pancreatic cancer cell lines. Percent-specific cytotoxicity was determined using the following formula: 100 × (experimental release − spontaneous release)/(maximum release − spontaneous release), and specific cytotoxic activity was calculated as follows: (cytotoxic activity in the presence of the peptide) − (cytotoxic activity in the absence of the peptide). Specific cytotoxicity of more than 10 % was considered to be positive.

Tetramer staining and flow cytometry

TAA-specific tetramers were purchased from Medical Biological Laboratories Co., Ltd. (Nagoya, Japan). Tetramer staining was performed as described below. One million isolated PBMCs or peptide-specific CTLs pulsed with TAA-derived peptides were washed, resuspended in 200 μl of PBS without calcium or phosphate, and stained with 40 μg/ml tetrameric complexes and monoclonal antibodies against cell surface proteins for 30 min at room temperature. The following monoclonal antibodies were used: anti-CD8-APC (BD PharMingen, San Diego, CA), anti-CCR7-FITC, anti-CD45RA-PerCP, and tetramer-PE. Cells were washed, fixed with 0.5 % paraformaldehyde/PBS, and analyzed on a Becton–Dickinson FACSAria II system.

Statistical analysis

Fisher's exact test and unpaired Student's *t* test were used to analyze the effect of variables on immune responses in pancreatic cancer patients. Overall survival was calculated from the day of pancreatic cancer diagnosis until the date of death or the last day of the follow-up period. Cumulative survival proportions were calculated using the Kaplan–Meier method, and any differences were evaluated using the log-rank test. A p value of <0.05 was considered to be significant, and all the tests were two-sided. All statistical analyses were performed using the SPSS statistical software program package (SPSS version 11.0 for Windows).

Results

Patients

Patient characteristics are summarized in the Supplementary Table. The median age of patients was 72 years, and patients included 24 males (59 %). The main localization of the tumors was the pancreatic head in 39 % of patients and the pancreatic body or tail in 61 %. The majority of patients (93 %) had advanced-stage cancer, namely, UICC stage III or IV. Therapeutic procedures mainly involved chemotherapy consisting of protocols such as gemcitabine monotherapy, S-1 monotherapy, or a combination of both drugs. Only 11 patients received the best supportive therapy to relieve physical and spiritual pain. A total of 61 % of patients had died by the last day of the follow-up period, and the median overall survival time of patients was 7.2 months.

TAA expression in pancreatic cancer cell lines and human cancer tissues

We evaluated the expression of 17 different TAAs in 9 human pancreatic cancer cell lines using real-time PCR. Although differences were observed from cell to cell, TAAs were expressed in more than 40 % of pancreatic adenocarcinoma cell lines, except for adenocarcinoma antigens recognized by T cells (ART)1 (11 %) and ART4 (33 %) (Table 2). We then investigated TAA expression in 7 surgical and 5 autopsy specimens. The expression of most TAAs in pancreatic adenocarcinoma specimens was similar to or more frequent than that in human pancreatic cancer cell lines, except for melanoma-associated antigen (MAGE)-A1 and MAGE-A3 (Table 2).

Detection of TAA-specific T cells by IFN-γ ELISPOT analysis

IFN-γ ELISPOT responses were evaluated with PBMCs to determine how frequently T cells respond to TAA-derived peptides and control peptides in patients with pancreatic adenocarcinoma (Fig. 1a). Positive responses to at least one TAA-derived peptide were observed in 28 of 41 (68 %) patients. On the other hand, 14 of 23 (61 %) peptides were recognized by T cells obtained from at least one patient. $ART1_{188}$, $ART4_{161}$, $ART4_{899}$, lymphocyte-specific protein tyrosine kinase $(Lck)_{208}$, $MAGE\text{-}A3_{195}$, $p53_{161}$, human telomerase reverse transcriptase $(hTERT)_{461}$, $hTERT_{324}$, Wilms tumor $(WT)\text{-}1_{235}$, vascular endothelial growth factor receptor $(VEGFR)2_{169}$, and $VEGFR1_{1084}$ were recognized in more than two patients, which suggested that these peptides have the potential to be immunogenic. Peptides 24 ($HIVenv_{584}$) and 25 ($CMVpp65_{328}$) were recognized in 0 and 38 % of patients, respectively.

Peptides $ART4_{161}$, $ART4_{899}$, Cyclophilin B $(Cyp\text{-}B)_{315}$, Lck_{208}, $hTERT_{324}$, and $VEGFR1_{1084}$ were recognized in more than one healthy volunteer, and/or the percentage of positive responses was higher in healthy volunteers than in pancreatic adenocarcinoma patients, which indicated

Table 2 Expression of various TAAs mRNA in pancreatic cancer cell lines and pancreatic cancer tissues measured by real-time PCR

TAA	Primer	Positive cell lines/ cell lines tested *n* (%)	Positive specimens/ specimens tested *n* (%)
ART1	Hs00188841_m1	1/9 (11)	5/12 (42)
ART4	Hs00221465_m1	3/9 (33)	11/12 (92)
CypB	Hs00168719_m1	9/9 (100)	12/12 (100)
Lck	Hs00178427_m1	8/9 (89)	11/12 (92)
MAGEA1	Hs00607097_m1	4/9 (43)	1/12 (8)
MAGEA3	Hs00366532_m1	4/9 (43)	1/12 (8)
SART1	Hs00193002_m1	9/9 (100)	12/12 (100)
SART2	Hs00203441_m1	9/9 (100)	12/12 (100)
SART3	Hs00206829_m1	9/9 (100)	12/12 (100)
HER2/neu	Hs00170433_m1	9/9 (100)	12/12 (100)
p53	Hs00153340_m1	9/9 (100)	12/12 (100)
MRP3	Hs00358656_m1	9/9 (100)	12/12 (100)
hTERT	Hs00162669_m1	9/9 (100)	9/12 (75)
WT-1	Hs00240913_m1	5/9 (56)	9/12 (75)
VEGFR2	Hs00911700_m1	5/9 (56)	11/12 (92)
VEGFR1	Hs01052961_m1	6/9 (67)	12/12 (100)
Survivin	Hs00153353_m1	9/9 (100)	12/12 (100)

that the responses to these peptides were not specific to T cells from patients with pancreatic adenocarcinoma (Fig. 1b). In other words, peptides $ART1_{188}$, MAGE-$A3_{195}$, $p53_{161}$, $hTERT_{461}$, WT-1_{235}, and $VEGFR2_{169}$ have specific immunogenic potential in patients with pancreatic adenocarcinoma.

The number of peptide-specific IFN-γ-producing T cells was counted to examine the frequency of T cells responsive to TAA-derived peptides. A range of 10–46 T cells per 300,000 PBMCs in patients with pancreatic adenocarcinoma produced IFN-γ (Fig. 1c).

TAA-specific CTL induction and cytotoxic activity

We attempted to induce peptides specific to CTLs from the PBMCs of pancreatic adenocarcinoma patients. Cytotoxicity assays were performed in more than five patients for each peptide. Of the 11 peptides recognized in more than two patients in the IFN-γ ELISPOT assay, 6 peptides (MAGE-$A3_{195}$, $p53_{161}$, $hTERT_{461}$, $hTERT_{324}$, WT-1_{235}, and $VEGFR2_{169}$) could induce their specific CTLs, which were confirmed to be able to respond to C1RA24 cells pulsed with corresponding peptides by the cytotoxicity assay, as shown in Fig. 2a.

We conducted a cytotoxicity assay to determine whether peptide-specific CTLs from healthy volunteers could show their cytotoxic activity against pancreatic carcinoma cell lines. $P53_{161}$-, $hTERT_{461}$-, and $hTERT_{324}$-specific CTLs showed cytotoxicity against YPK-2 (HLA-A24-, p53-, and hTERT-positive), but not against Panc-1 (HLA-A24-negative, p53- and hTERT-positive). MAGE-$A3_{195}$-, WT-1_{235}-, and $VEGFR2_{169}$-specific CTLs also showed cytotoxic activity against YPK-2 (HLA-A24-, MAGE-A3-, WT-1-, and VEGFR2-positive), but not against YPK-1 (HLA-A24-positive, MAGE-A3-, WT-1-, and VEGFR2-negative). Representative data are shown in Fig. 2b.

Phenotypic analysis of TAA-derived peptides specific to T cells

To analyze the characteristics of TAA-derived peptides specific to T cells and select the appropriate epitope for immunotherapy in patients with pancreatic adenocarcinoma, we performed phenotypic analysis by tetramer staining and FACS analysis. We first attempted to detect MAGE-$A3_{195}$-, $hTERT_{461}$-, and WT-1_{235}-specific tetramer-positive T cells in PBMCs and CTLs induced by the corresponding peptides in healthy volunteers. The ratio of tetramer-positive T cells was increased in CTLs and their frequencies were 1.481–2.930 % of $CD8^+$ T cells, suggesting that these tetramers work well (Fig. 3a). We also conducted similar assays in pancreatic adenocarcinoma patients and detected tetramer-positive T cells in CTLs (Fig. 3b).

We then examined the naïve/effector/memory phenotype of tetramer-positive cells in the PBMCs of patients. The memory phenotype was investigated by the criterion of CD45RA/CCR7 expression [28]. In tetramer analysis, the frequencies of MAGE-$A3_{195}$-, $hTERT_{461}$-, and WT-1_{235}-specific tetramer-positive T cells were 0.003–0.044,

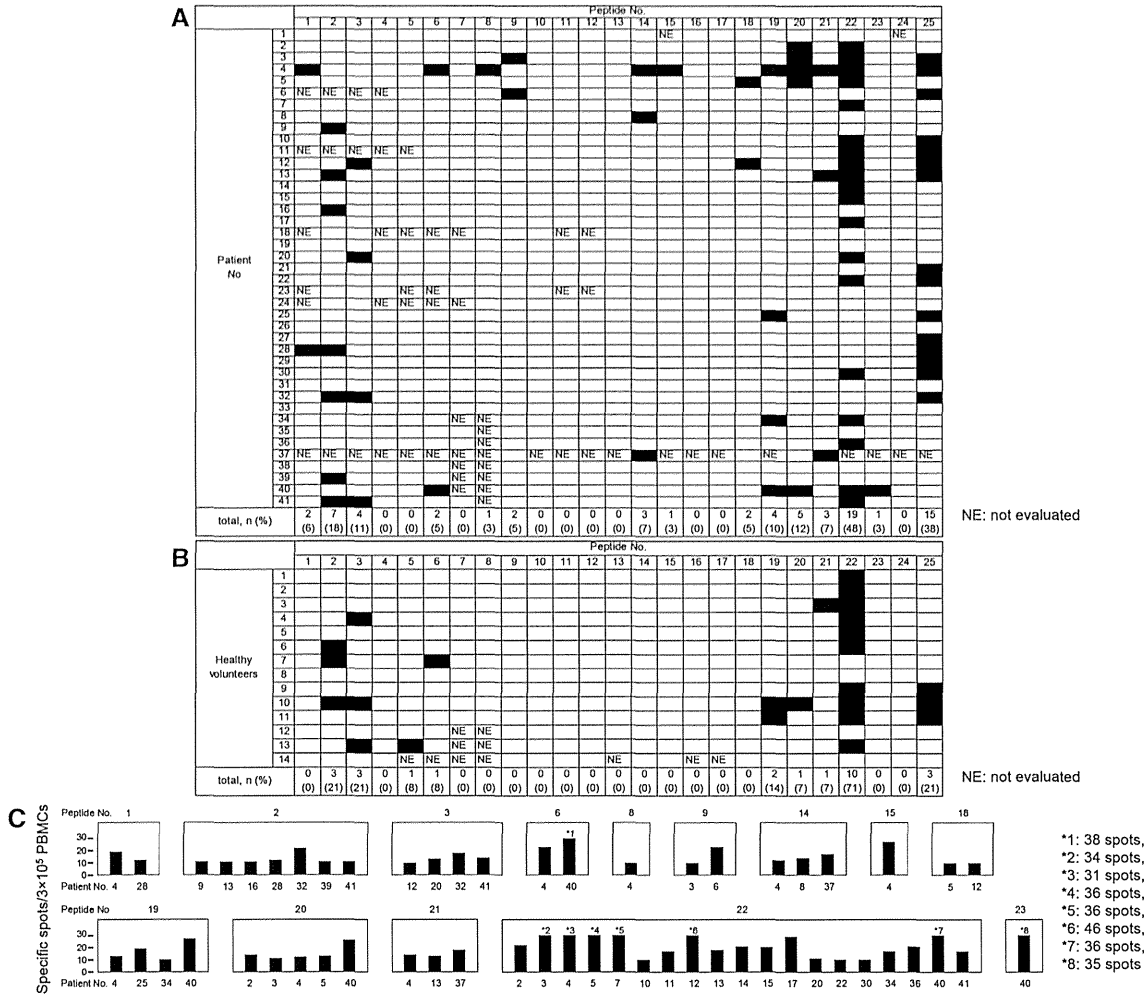

Fig. 1 T cell responses to TAA-derived peptides and control peptides in pancreatic adenocarcinoma patients **a** and healthy volunteers **b**. T cell responses were evaluated by the IFN-γ ELISPOT assay. Responses were considered positive if 10 or more specific spots were detected and if the number of spots in the presence of an antigen was at least twofold that in its absence. *Black boxes* indicate positive responses. **c** The frequency of TAA-specific IFN-γ-producing T cells evaluated by the ELISPOT assay. *Black bars* indicate the response of one patient

0.006–0.053, and 0.030–0.191 % of $CD8^+$ T cells, respectively. The frequency of $CD45RA^-/CCR7^+$ (central memory), $CD45RA^-/CCR7^-$ (effector memory), and $CD45RA^+/CCR7^-$ (effector) T cells in tetramer-positive cells depended on the patient and all phenotypes were observed in all patients, except for patients 1, 8, 28, 29, and 4 (Supplementary Fig. 1).

TAA-specific T cell responses and clinical features of pancreatic cancer patients

In the present study, we analyzed the clinical features that can affect TAA-specific immune responses. When we divided patients into two groups based on their frequencies of lymphocyte subsets in peripheral leukocytes (<24 %, the median value among all patients, or equal to or more than 24 %) and the strength of TAA-specific immune responses into three groups according to the frequency of TAA-specific T cells (<10 specific spots on ELISPOT assays, no response; 10–19 specific spots, weak response; equal to or more than 20 specific spots, strong response), the patients with more lymphocyte subsets in peripheral leukocytes showed stronger TAA-specific T cell responses (Supplementary Fig. 2). On the other hand, we could not find any relationship between TAA-specific immune responses and other clinical characteristics such as age, sex, tumor marker levels, UICC stage, or metastasis status.

We also analyzed the correlation between T cell responses and the prognosis of pancreatic cancer patients. The median overall survival time of patients with T cell responses to at least one TAA-derived peptide evaluated

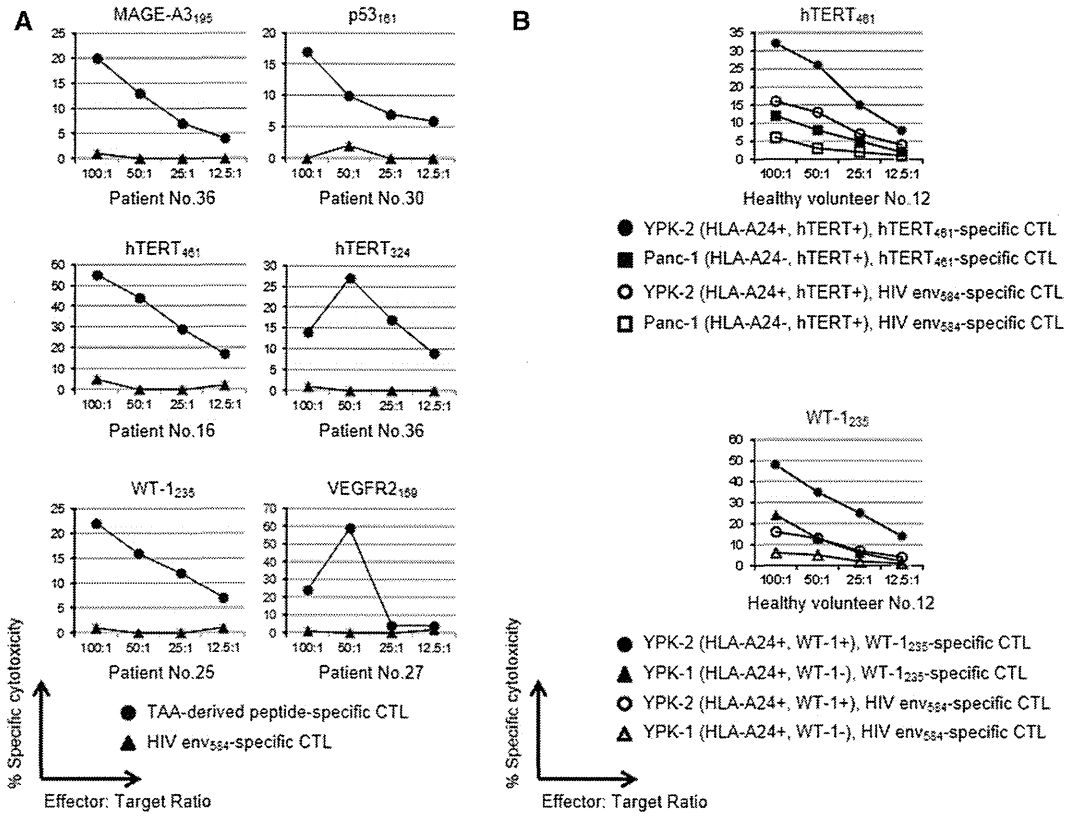

Fig. 2 **a** T cell responses to peptides evaluated by the cytotoxicity assay. Peptide-specific CTL induction and cytotoxicity assays were performed on the PBMCs from at least five patients, and representative data are shown when peptide-specific CTLs were induced in one or more patients. A percent-specific cytotoxicity of more than 10 % was considered to be positive. Six peptides: 9, 14, 18, 19, 20, and 21, could induce their specific CTLs, and these could respond to C1RA24 cells pulsed with the corresponding peptides in the cytotoxicity assay. **b** Cytotoxic activity against the pancreatic carcinoma cell lines of TAA-specific CTLs from healthy volunteers evaluated by the cytotoxicity assay. Cytotoxicity was stronger against pancreatic carcinoma cells that were HLA-A24-restricted and expressed corresponding TAAs than against those not HLA-A24-restricted or not expressing corresponding TAAs

by the ELISPOT assay was 12.2 months, which was significantly longer than that without T cell responses (4.3 months) ($p = 0.013$) (Fig. 4a). On the other hand, no correlation was observed between positive T cell responses and CMV-derived peptides and clinical outcomes (Fig. 4b), suggesting that TAA-specific T cell responses, but not the general immune response, is a prognostic factor in patients with pancreatic adenocarcinoma. The frequencies of regulatory T cells or the ratio of regulatory T cells to $CD8^+$ T cells had no impact on the outcomes of patients in this study.

Discussion

Immunotherapy is considered to be a fourth treatment procedure for cancer following surgical resection, radiotherapy, and chemotherapy [29]. Cancer vaccine therapy was previously shown to convey survival benefits to prostate cancer patients in a clinical phase III trial [30], and some candidates of other cancers have been identified and separately evaluated to determine whether a CTL response can be elicited, with the subsequent elimination of cancer cells and improvement in outcomes. Although a successful clinical response depends on how much tumor antigens elicit their specific CTLs, which are the most important effector cells for antitumor immune responses, to the best of our knowledge, no studies have attempted to identify which epitopes are optimal for peptide vaccine therapy in patients with pancreatic adenocarcinoma. Therefore, we simultaneously compared peptide-specific T cell responses among various TAAs in 41 identical patients with pancreatic adenocarcinoma under the same experimental conditions.

Therapeutic function is the most important factor to consider when determining the usefulness of cancer antigens for peptide vaccine therapy. However, it is very difficult to compare the efficacy of more than one epitope, especially in patients with pancreatic adenocarcinoma whose survival time is very short. Under such circumstances, immunogenicity, specificity, oncogenicity, expression levels, % of

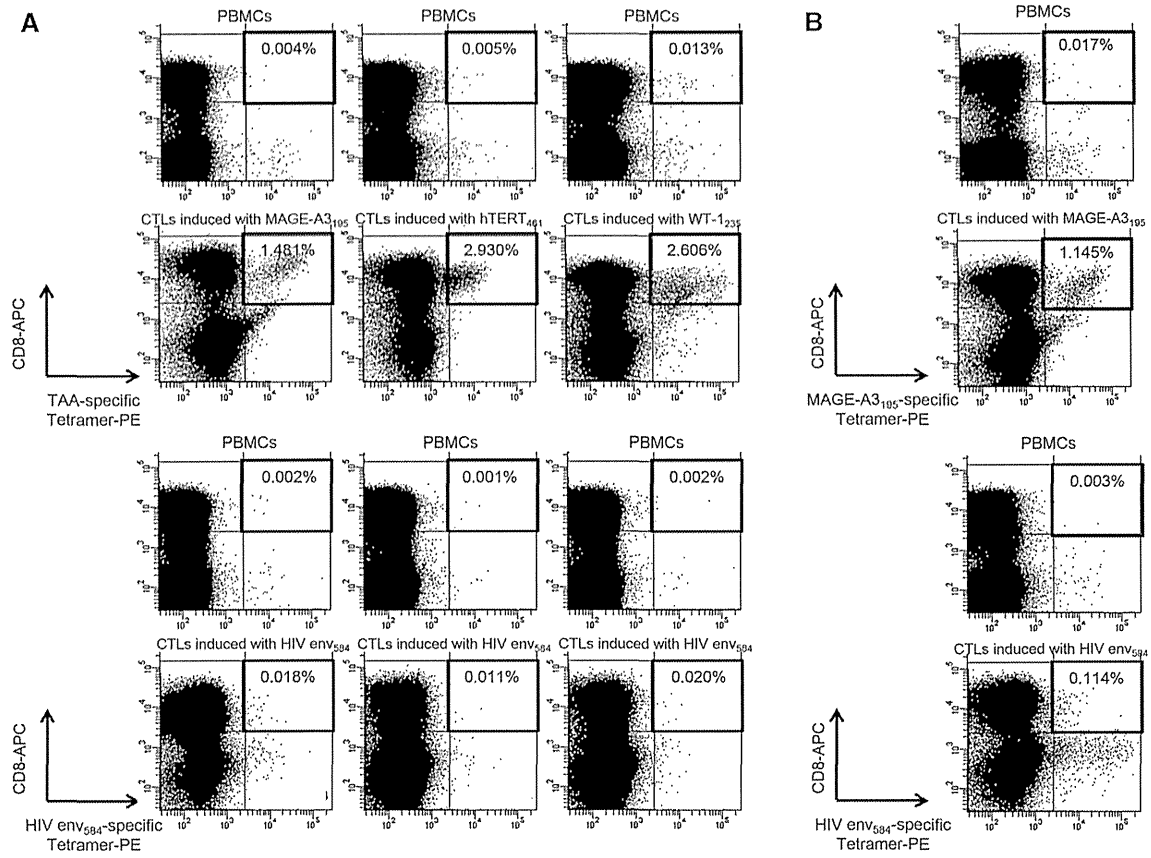

Fig. 3 Detection of TAA-specific, HLA-A24-tetramer$^+$, and CD8$^+$ lymphocytes in PBMCs from healthy volunteers and pancreatic adenocarcinoma patients. **a** Tetramer analyses were performed on eight healthy volunteers for each peptide (MAGE-A3$_{195}$, hTERT$_{461}$, and WT-1$_{235}$). Tetramer$^+$ and CD8$^+$ T cells were detectable in both PBMCs and CTLs induced by their corresponding peptides in at least one healthy volunteer, and representative data are shown in cases in which the ratio of tetramer$^+$ and CD8$^+$ T cells to CD8$^+$ T cells was higher in CTLs induced with each TAA-derived peptide than in PBMCs. **b** Tetramer analyses were performed on pancreatic adenocarcinoma patients using PBMCs and CTLs, which were induced with TAA-derived peptides and showed cytotoxicity against pancreatic cancer cell lines in cytotoxicity assay. Levels of tetramer$^+$ and CD8$^+$ T cells were higher in CTLs induced with TAA-derived peptides than in PBMCs. Representative data are shown in cases in which the ratio of tetramer$^+$ and CD8$^+$ T cells to CD8$^+$ was 0.017 % in PBMCs and 1.145 % in MAGE-A3$_{195}$-specific CTLs

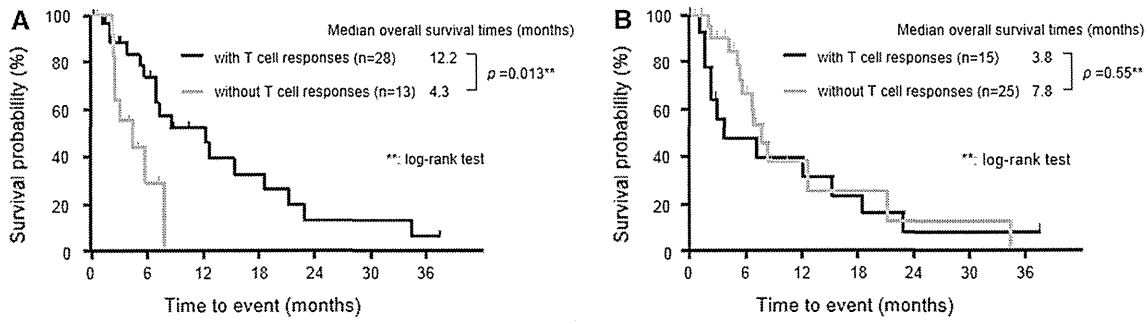

Fig. 4 Kaplan-Meier plot of the overall survival of pancreatic cancer patients according to **a** TAA-specific T cell responses and **b** T cell responses to CMV-derived peptides. **a** TAA-specific T cell responses were defined as positive if 10 or more specific spots to at least one TAA-derived peptide were detected on the ELISPOT assay. The overall survival time of patients with TAA-specific T cell responses was significantly longer than that of patients without TAA-specific T cell responses. **b** T cell responses to CMV-derived peptides were defined as positive if 10 or more specific spots to CMV-derived peptides were detected on ELISPOT assays. No correlation was observed between positive T cell responses to CMV-derived peptides and the clinical outcomes of patients